Medjunarodni naučno-stručni skup sa izložbom
XXIII NAUKA I MOTORNA VOZILA 2011
SCIENCE AND MOTOR VEHICLES
International Automotive Conference with Exhibition
19 - 21 April 2011, Beograd, Serbia

NMV11SAF15

Preliminary design of a magnetorheological brake for automotive use

Marannano G. V.[1]; Virzì Mariotti G.[1], Duboka Č.[2];
[1]*Dipartimento di Meccanica Università di Palermo, Italia*
[2]*University of Belgrade, Faculty of Mechanical Engineering, Serbia*

Abstract
After an initial study of the characteristics of magnetorheological fluids based on a thorough search in literature, a preliminary configuration of MR brake is proposed. It comes from the evaluation of the main factors influencing the design of an appropriate magnetic circuit, and then the performance obtained in terms of brake torque. The analytical study of the brake has allowed a first preliminary sizing. Through the subsequent execution of an electromagnetic finite element model, created in ANSYS, it was possible to assess more accurately the distribution of the magnetic field inside the MR fluid and hence the resistance to relative motion between rotor and stator. The work needs an accurate optimization due to insufficient value of the braking torque and high mass of the device.

Key words – Magnetorheological fluids; MR brake; Magnetic FEM

1. Introduction.

In recent years, due to a strong technological development, there has been a gradual increase in the presence of electronics in the engineering industry and especially in the field of motor vehicles.
The use of electrical and electronic components in vehicles has improved their performance with significant reductions in production costs and increase of both active and passive safety. So called X-by-wire technology provides for the future the development of electromechanical vehicle systems control, such as steering, gearbox, clutch accelerator. Today's EBS - Electronic Braking Systems, for example, allow better braking performance in terms of deceleration or stopping distance, but also better stability of a vehicle during braking. At this stage, EBS only provides electronic transfer of the braking control, while wheel brakes are still friction mechanisms with non/electronic control, like mechanic, or hydraulic, or pneumatic.
Magneto-Rheological Brake (MRB) is one of the possibilities to replace a friction brake in an EBS with a brake in which Magneto-Rheological Fluid (MRF) is interposed between a rotor and a stator. These fluids are known in the literature as-Controllable Fluids (CF) to emphasize the characteristic of being governed in their rheology, if crossed by a magnetic field. The main advantage that characterizes them is the ability to respond in a simple, quiet and quick way to external controls. They also have the ability to provide a quick and simple interface between the electronic control and mechanical system. MR fluids belong to the category of materials defined in the literature as "smart materials" or "intelligent materials". In the event of absence of magnetic field, the fluid behaves like a liquid, having viscosity comparable to that of oil, while it is transformed into solid gel due to its magnetization. The transition from one state to another is abrupt and occurs in a few milliseconds. The implementation of MR device requires the design of the magnetic circuit (Carlson, November 1999; Brauer, 2006), like this paper reports.

.

MR fluids have been the subject of numerous studies and patents (Rabinow, 1951; Carlson, Catanzarite and Clair, 1996; Carlson et al., 1998; Foister, 1997; Jolly, Bender and Carlson, 2000; Ly et al. 1999; Genc and Phulé 2002; Carlson, 2001, dec, 1999; Jolly,Carlson and Munoz,. 1996; Farjoud, Vahdati and Fah, 2008; Klingenberg, 2001; Olabi and Grunwald, 2007) their application affects a number of mechanical components used in cars and other devices, such as, clutches (Gopalswamy, 1998; York, 1997; Kavlicoglu et al., 2002; Benetti and Dragoni, 2006; Jaindl et al. 2007) and valves (Grunwald and Olabi, 2008; Yang, Duan and Eriksson, 2008; Li, Du and Guo, 2003; Nguyen, Choi and Wereley, 2008). The use of MR fluid dampers for motor vehicles (Dogrouz et al., 2003) allows the construction of suspension at variable calibration with obvious advantages for the vehicle's dynamic behavior (Virzì Mariotti, Lopez and Triscari, 2002; Gillespie, 1992), it seems that the use of MR suspension (Barbaraci and Virzì Mariotti, 2009) is better than electrorheological suspension (Filisko and Henley, 1999), the features are still under investigation. Besides, MR fluids oppose certain resistance to sliding, and have the ability to control the amount of shear stress, which suggests their application in a brake, which represents the objective of this work. In the literature many papers are found (Karakoc, Park and Suleman, 2008; Benetti and Dragoni, 2006; Yang, Huang and Kang, 2007; Li and Du, 2003; Liu et al., 2006).

Paper (Liu et al., 2006) contains the design of a MR brake with FEM analysis and experimental tests that that prove a hysteretic behaviour; paper (Karakoc, Park and Suleman, 2008) reports the design, the optimization and experimental tests of a MR brake, with the conclusion that the brake is not sufficient to stop the vehicle , paper (Li and Du, 2003) shows the results of the experimental test on a MR brake, concluding that the torque increase with the increase of the magnetic field until the saturation, designing the electromagnet at high efficiency by FEM. The main advantages of MR brakes are a more rapid response in operation and reduction of the number of braking system components. Their disadvantages are high mass of the device and the lack of sensitivity in braking; the papers containing a survey on the disadvantages are very few. The development of brake begins looking at the main brake operation factors by which MR brake could achieve performance comparable to that of a conventional automotive brake [f.e. Aleksendrić et al., 2006; Aleksendric, Duboka and Virzi' Mariotti, 2008). Particular attention is put to the choice of an appropriate configuration of the magnetic circuit to obtain the magnetization of the fluid and to generate the required braking torque. In particular a system with four active surfaces is designed in order to reduce the mass and the radial size and increase the braking torque. The possibilities offered by this type of system are assessed by the implementation of a preliminary analytical model and the subsequent execution of an electromagnetic Finite Element (FE) calculation that simulates the operation of the device. This paper shows that the preliminary design is not able to implement a brake able to stop the vehicle and that the brake has a too high mass for a practical application; the second part shows that an accurate optimization can eliminate the disadvantages, and also that the thermal problem (Wiehe, Noack and Maas, 2009) has high importance.

2 MR brake

The change of viscosity of MR fluid is used to generate a viscous force between two discs, in relative motion, separated by a cavity, as shown in (Fig. 1) Assuming that one disk is stationary while the other is rotating with an angular velocity ω, the expression of shear stress "τ" is given by Bingham (Rabinow, 1951; Carlson et al., 1996):

$$\tau = \tau(H) + \eta \cdot \dot{\gamma} \tag{1}$$

Where "τ(H)" is the tangential stress due to the only variation of the magnetic field intensity H, η is the viscosity of the fluid and "$\dot{\gamma}$" is the tangential velocity gradient. Assuming a small gap ξ of fluid, it is:

$$\dot{\gamma} \cong \frac{\omega \cdot r}{\xi} \tag{2}$$

where r is the generic radius of the disk. Considering an infinitesimal element of area on the disc surface equal to $dA = r \cdot d\theta \cdot dr$, where r and θ are the polar coordinates, which is subject to the shear stress τ, the

elementary torque dT transmitted at distance r by the rotation axis is (Karakoc et al., 2008) (Yang et al., 2007):

$$dT = \tau \cdot dA \cdot r = \tau \cdot r^2 \cdot d\theta \cdot dr \tag{3}$$

Substituting the relationship (6) and integrating over the disk surface, one obtains:

$$T = \int_{0}^{2\pi}\int_{r_i}^{r_e} \left[\tau(H) + \frac{\eta \cdot \omega \cdot r}{\xi} \right] \cdot r^2 \cdot d\theta \cdot dr = 2\pi \int_{r_i}^{r_e} \left[\tau(H) + \frac{\eta \cdot \omega \cdot r}{\xi} \right] \cdot r^2 \cdot dr \tag{4}$$

It can be written as a sum of two terms:

$$T_H = 2\pi \int_{r_i}^{r_e} \tau(H) \cdot r^2 \cdot dr \tag{5}$$

$$T_\eta = \frac{\pi}{2} \cdot \frac{\eta}{\xi} \cdot \omega \cdot (r_e^4 - r_i^4) \tag{6}$$

where T_H and T_η are the torque components due respectively to the applied magnetic field and to the viscosity of MR fluid; while the significance of the second term is negligible compared to the first. Equation (5) shows that the braking torque is a function of geometrical dimensions and of the magnetic field intensity H.

2.1 Design of magnetic circuit

Magnetic circuit generates an appropriate magnetic field in the MR fluid (Carlson, Nov. 1999; Brauer, 2006). Fig. 2 shows a simple draw of the electromagnetic circuit, which can be used as a reference for the analysis and design. The magnetic circuit consists of a ferromagnetic material having shape of C and a gap of height ξ that contains the MR fluid. Surfaces A_f in contact with the fluid, represent the active surfaces of the device.

The magnetic flux ϕ, whose lines are shown in figure 2, is generated by a coil constituted by N turns. Electromagnetic circuit design requires the choice of the working point of MR fluid (H_f, B_f), which provides the desired value of yield stress τ_y. The total magnetic flux through the fluid is:

$$\phi = B_f \cdot A_f \tag{7}$$

Magnetic flux is constant in each section for the principle of continuity, so that the magnetic field B_s, in the generic branch s of the circuit, having section A_s, is given by:

$$B_s = \frac{\phi}{A_s} = B_f \cdot \frac{A_f}{A_s} \tag{8}$$

The working point can be determined from the B-H characteristic of the ferromagnetic material. The necessary number of Amp-turns to obtain the required value of B_f in the gap can be obtained applying Ampere's theorem: the value of H circulation on a closed curve Z equals the current flux outgoing across surface S that Z curve contains, i. e:

$$\oint_Z \vec{H} \cdot d\vec{L} = \int_W \vec{J} \cdot d\vec{W} \tag{9}$$

Remaining within the limits of linearity, the permeability μ of both magnetic material and MR fluid can be considered constant. Under these conditions one can write:

$$H = \frac{B}{\mu}$$ (10)

and substituting the relationship (8) into (10) one has:

$$H_s = \frac{\phi}{\mu \cdot A_s} \qquad H_f = \frac{\phi}{\mu \cdot A_f}$$ (11)

Ampere's theorem can be written in the form:

$$N \cdot I = H_f \cdot \xi + \sum H_s \cdot L_s$$ (12)

L_s is the length of the s-th branch of the circuit and ξ is the thickness of gap of fluid. Introducing also the reluctance:

$$\Re = \oint_Z \frac{dL}{\mu \cdot A}$$ (13)

Ampere's theorem (12) becomes:

$$\oint_Z \vec{H} \cdot d\vec{L} = \phi \cdot \int_Z \frac{dL}{\mu \cdot A} = N \cdot I$$ (14)

and ultimately one can write:

$$N \cdot I = \phi \cdot (\Re_f + \Re_s) = \phi \cdot \left(\frac{\xi}{\mu_f \cdot A_f} + \sum \frac{L_s}{\mu_s \cdot A_s} \right)$$ (15)

in which $\Re_f$ e $\Re_s$ indicate respectively the reluctance of the gap fluid and one of the parts of the circuit in ferromagnetic material. The product $N\,I$ is named magnetomotive force *mmf* of the magnetic circuit. Minimization of the total reluctance of the circuit is important to minimize the number of Amp-turns. Generally the parts in ferromagnetic material contribute little to the overall value of the reluctance of the circuit. In fact the materials used to make magnets have a permeability that is several thousand times greater than that of the vacuum, while the permeability of MR fluid takes up a value of about 9 times μ_0. Thus, in first approximation, the Ampere's law that regulates the system can be written:

$$N \cdot I = \phi \cdot \frac{\xi}{\mu_f \cdot A_f} = B_f \cdot \frac{\xi}{\mu_f}$$ (16)

Weight of the ferromagnetic circuit must not affect too much the total weight of the device. To reduce the weight, the sections A_s, in every branch of the circuit, must be reduced, but without changing the work point of the fluid. Since the flow is constant in each branch, the values of the magnetic field can be increased, but the complete saturation of the entire section must not occur. In correspondence of a value of magnetic field near to the saturation value, there is a gradual decrease of the magnetic permeability of the material (slope of

the B-H curve), with an increase of the reluctance $\mathfrak{R}_s$ of ferromagnetic material, and of the total reluctance of the circuit.

2.2 Configuration and material selection.

Figure 3 shows a schematic cross section of the basic model of the proposed brake. The model consists of a rotor comprising a hollow input shaft (1), to which two discs (2) are rigidly connected, and a stator, constituted by an outer cylindrical case in two parts (3) and (4), which houses the electromagnetic coil (5). A third hard drive (6) is linked to the outer case and is interposed between the rotor discs; it is held in position by a support ring (7). The axial cavity, thus created between the discs and the stator, contains the MR fluid (8). Four active surfaces are in contact with the MR fluid, in order to obtain a good compromise between the achievement of sufficient braking torque and simple construction and assembly of the device.

Contact area between disc and MR fluid is the active surface, on which the shear stresses act, opposing the relative motion. The braking torque is calculated by integrating the stresses over the entire active surface. In general an increase in the size of the active surface can increase the achievable performance in terms of torque. However, this increase cannot be arbitrary, both for reasons of excessive volume and for the fact that an increase of area *A* leads to a lower magnetic induction *B*, and to a reduction of shear stress transmitted by the MR fluid.

The choice of appropriate materials in the design of the brake has a key role both in terms of performance (torque output) and in terms of geometry (weight and size). Each component of the brake, crossing by the magnetic flux, must have a ferromagnetic behaviour ($\mu_r \gg 1$). The material of the other parts may be chosen on structural and thermal considerations. The selection of a suitable ferromagnetic material is based on certain characteristics as:
- High coefficient of permeability
- High value of saturation of magnetic induction
- Low hysteresis energy loss
- Permeability should remain substantially constant with magnetic field and temperature variations.

Choice of the MR fluid has special relevance, because the magnetic and rheological properties greatly influence the performances of the brake. To obtain low values of the ratio weight/braking torque, the fluid has to be capable of transmitting high shear stresses with low values of magnetic induction. Discs (2) and (6) and part of the outer stator (3) must be made of ferromagnetic material, as part of the magnetic circuit. Non-magnetic materials are used for the remaining parts in order to avoid spreads in areas where the flow is not necessary. Chosen MR fluid is MRF-140CG, produced by LORD Corporation; the curves for their magnetic and rheological properties are reported in Figures 4 and 5, while table 1 shows the main physical properties.

Magnetic circuit has been achieved with simple carbon steel C10 (ISO 683-11), which has good ferromagnetic properties combined with excellent mechanical strength. For components not part of the magnetic circuit, material selection is solely based on considerations regarding density, mechanical and thermal properties. In particular, the input shaft is made of stainless steel AISI-304; in order to significantly reduce the mass of the brake and favour the loss of heat, the remaining parts are made in aluminium alloy T6061-T6 Al. Fig. 6 shows B-H curve of ferromagnetic material C10, while Table 2 shows the main physical and mechanical properties of selected materials for the development of the brake.

2.3 Preliminary Design

By the previous, an approximate analytical report may be derived in order to obtain a preliminary sizing of the model, setting particular attention to the design of the magnetic circuit (Karakoc, Park and Suleman, 2008; Yang, Huang and Kang, 2007). Assuming that the brake has four active surfaces and by making the simplifying assumption that the magnetic field, and the shear stress, remains constant along the active surface of the fluid at different distances from the axis of rotation, the equation (5) of the braking torque becomes:

$$T = \frac{8}{3}\pi \cdot \tau(H) \cdot (r_e^3 - r_i^3) \cdot \lambda \qquad (17)$$

r_i and r_e represent respectively the outer and inner radius of each disc in contact with the MR fluid (surface active); λ is a correction coefficient that takes into account the simplifying assumptions in the calculation of the magnetic field. In the choice of an appropriate value of r_e, the presence of additional elements outside the disc has to be taken in account. Particularly important is the ring separation in aluminium between fluid and coil. It provides support to the stator disk and thus its reduced thickness may be cause of structural problems, as well as difficulties in construction and assembly. By (17), the value of tangential stress can be calculated, so that magnetic induction H and magnetic field can be calculated by fig. 4 and 5.

Simplifying assumption of negligible reluctance of the parties in ferromagnetic material, the magnetomotive force can then determined by (16).

3 Finite element analysis of MR brake
3.1 Objectives

The analytical study of the MR brake has highlighted the close relationship between the shear stress in the fluid, depending on the magnetic field, and the benefits obtained in terms of generated braking torque. The result can be improved by applying the magnetostatic finite element analysis. FEM analysis eliminates many simplifications assumed in the sizing of the magnetic circuit. The accuracy of the study is mainly due to the possibility of considering the actual non-linear magnetic properties of materials and the inevitable loss of flow in the circuit, due to its reluctance. Thus the intensity of the magnetic field is assessed in a more precise way and its variation along the active surface is taken in consideration. The magnetic field lines have the perpendicular direction to the relative slippage surface; this condition is necessary for the working of the device in shear mode.

3.2 Magnetic Analysis

ANSYS allows to analyze the distribution of magnetic field by Maxwell's equations for static, time-independent analysis:

$$\nabla \times H = J \qquad \nabla \cdot B = 0 \qquad (26)$$

in which J indicates the current density vector. The resolution of these equations, on a domain defined by appropriate boundary conditions, allows the assessment of the value of the magnetic field B and of the values of magnetic intensity H. The magnetostatic analysis is conducted through the use of ANSYS in batch mode; a trace file is created, which provides to the sequence of instructions to perform, both in creation of model analysis and in visualization of results (pre and post processing), by using the internal programming language APDL (ANSYS Parametric Design Language). The approach used is rather onerous in terms of achievement, but it has the significant advantage of allowing quick changes to the model for conducting further analysis, as required by the optimization process.

The first aspect to consider in creating FE model is the choice of a geometry that represents accurately and simply the system. Because the MR brake has an axial symmetry, it can be studied with an axialsymmetric model. Plane13 is a quadrilateral four-node plane element characterized by four degrees of freedom, including the component of the magnetic potential vector A. The option of axial symmetry (KEYOPT (3) = 1) can be also activated for this element. The model is characterized by a regular quadrilateral mesh, fairly thick in the thickness of MR fluid, this is a necessary condition for high accuracy of results in areas of interest. Figure 8 shows the geometry of the FE model. Figure 9 shows the same pattern in three-dimensional visualization.

Magnetic materials are characterized by absolute magnetic permeability μ as function of applied magnetic field. μ value decreases increasing magnetic field until the saturation value B_{sat}, at which one has $\mu = \mu_0$ ($\mu_r = 1$).

The slope of BH curve is equal to the value of absolute permeability ($\mu = \partial B/\partial H$). In particular, it was derived from the ANSYS library materials for steel C10 (Figure 6), while it was referred to the B-H curve shown in figure 5 for the MR fluid. Relative magnetic permeability has been considered constant and equal to $\mu_r = 1$ for non-magnetic materials.

The boundary conditions of the model mainly concern the loads applied and the constraints. Acting load is represented by the intensity of current through the coil that generates the magnetic field in the brake. It was introduced in the FE model by defining the current density $J = NI/A$ corresponding to the elements representing the winding. The model is also constrained with no component of magnetic potential vector A_z, on the nodes at the outer boundary. This implies that the magnetic flux lines are maintained in a direction parallel to the outer contour lines.

The solution is obtained through an iterative-incremental process, to take into account the nonlinear characteristics of materials. Non-linear analysis requires the gradual load application, thus promoting the convergence of the solution. Five substeps are used, each of which the current density is increased gradually, to obtain an accurate estimate of the magnetic field.

3.2.1 Postprocessor

The phase of postprocessor returns the results of the magnetostatic analysis and allows the subsequent processing. To estimate the generated braking torque, an automatic sequence of operations was set using the programming language APDL. The value of magnetic induction H, along its radial coordinate is obtained on every node of the contact surface between the disc and MR fluid. For each value of H, the corresponding value of shear stress is determined by interpolation of the curve τ-H characteristic of MR fluid.

The braking torque T_H is obtained multiplying relationship (5) by the number n = 4 of active surface; the integral can be approximated by the following relationship:

$$\int_{r_i}^{r_e} \tau(H) \cdot r^2 \cdot dr \cong \sum_{j=1}^{n_1} (r_{j+1} - r_j) \cdot \tau_j(H) \cdot r_j^2 \qquad (27)$$

where r_j is the radial coordinate of the j-th node and n is the total number of nodes in every active surface. Resulting braking torque is calculated by taking into account only the contribution of τ_H, caused by the magnetization of the fluid, while the contribute due to the viscosity of the fluid is considered negligible. The weight of the model is obtained by an additional routine, by calculating the volume of each element and multiplying by the density.

3.3 Results

FEM analysis conducted on the model returns the distribution of magnetic field. The flow lines shown in Figure 10 are very close to those shown in Figure 7. They follow the path along the stator in ferromagnetic material, going to cross the four gap of fluid in the perpendicular direction to the flow direction. The latter is detectable by magnification shown in Figure 11, corresponding to the active surfaces.

Figure 12 shows the map of the values obtained for the magnetic field B in the circuit. Figure 13 shows instead the distribution of the magnetic field represented by vectors. The highest values of magnetic field are achieved in the stator in the nearness of the winding. In these areas the steel supports values of B very near to the saturation value, as expected, confirming the preliminary sizing. It also confirms the need to consider the actual magnetic behaviour of steel, taking into account the nonlinearity near to its saturation point. Magnetic field over four fluid gap is less than calculated $B_{f,\max} = 0,6\,T$ with preliminary sizing. This is clarified by considering the B-H curve of steel C10 (Figure 6): not negligible values of magnetic field intensity correspond to high values of magnetic induction.

Figure 14 shows the values of magnetic field intensity in the brake circuit. In correspondence of the active surfaces of fluid, the value of H is smaller than the calculated value $H_f=75kA/m$ on the basis of simplifying assumptions (negligible reluctance of the stator).

According to (Karakoc, Park and Suleman, 2008), the shear stress $\tau(H)$ is insufficient to generate adequate braking torque. For the geometry used in the preliminary analysis a value equal to $T = 784{,}53\ Nm$ is estimated. It should be noted that the transmission of the required braking moment $T_{nom} = 1036\ Nm$, which calculation is reported in the appendix, can be obtained only after an accurate optimization process.

The mass of the brake model has been calculated easily by the numerical simulation and has the value $m_b=42{,}25\ kg$. The value is excessive as it seriously compromises the comfort of march (Genta, 2002; Gillespie, 1992), if the brake is part of the unsprung mass; the last would increase of 170 kg approximately.

The obtained results show that the successive process of optimization is necessary and aims at the improvement of the two obtained result: that one to increase the braking moment and that one to reduce the mass. Moreover it is necessary to verify that the temperature in exertion does not compromise the characteristics of MR fluid.

4. Conclusions

The purpose of this work is to study the potential use of MR fluid to design a vehicle brake.

MR brake consists of a rotor and a stator with two discs containing the electromagnetic coil. The gap between stator and rotor is filled with MR fluid. Thus is created the necessary magnetic circuit for proper magnetization of the fluid and the required braking torque. The preliminary configuration of brake fluid is obtained by the evaluation of the main factors influencing the design of magnetic circuit, and the performance obtained in terms of brake torque. Through the subsequent realization of a finite element electromagnetic model it was possible to assess more accurately the distribution of the magnetic field inside the MR fluid and the resistance to relative motion between rotor and stator.

FEM analysis has shown that the preliminary sizing is not sufficient to implement the brake, because the braking torque is in reality lower than the design value. The analysis of the model highlights the possibility of changing the geometrical parameters, appropriately altering the magnetic circuit in order to obtain benefits comparable to those of a conventional vehicle brake in term of braking torque. Considering the number of parameters involved (size of active surfaces, geometry of the stator coil size) and the existence of a close relationship between them, their modification can not be changed arbitrarily.

It is deemed necessary to follow a scientific approach to seeking the optimal parameters, based on results of further analysis conducted on the model, such as the optimization process.

References

Aleksendrić D., Duboka Č., Gotowicki P. F., Nigrelli V., Virzì Mariotti G., 2006, "Braking Procedure Analysis of a Pegs-Wing Ventilated Disk Brake Rotor" Int. J. Vehicle Systems Modelling and Testing, Vol. 1, No 4, pp 233-252

Aleksendrić, D., Duboka, Č., Virzì Mariotti, G., 2008, "Neural Modelling of Friction Material Cold Performance" Proceedings of the Institution of Mechanical Engineers, Part D: Journal of Automobile Engineering, Volume 222, Issue 7, Pages 1201-1209

Barbaraci, G; Virzì Mariotti, G., 2009 "The Recovery of the Optimal Damping Constant by the MRF Damper" Mobility and Vehicle Mechanics, RS, vol. 35, n. 4, December, pp. 1-17, ISSN: 1450-5304.

Benetti, M., Dragoni, E., 2006, "Nonlinear Magnetic Analysis of Multi-plate Magnetorheological Brakes and Clutches", Excerpt from the Proceedings of the COMSOL Users Conference, Milano.

Brauer, J.R., 2006, "Magnetic Actuators and Sensors" John Wiley & Sons.

Carlson, J.D. et Al. 1998,, "Controllable brake", US Patent 5,842,547, Lord Corporation.

Carlson, J.D., November 1999, "Magnetic Circuit Design", Engineering note, Lord Corporation, Materials Division.

Carlson, J.D., December 1999, "Designing with MR fluids", Engineering note, Lord Corporation, Materials Division.

Carlson, J.D., 2001, "What makes a good MR Fluids?", 8th International Conference on Electrorheological (ER) Fluids and Magnetorheological (MR) Suspensions, Nice, July.

Carlson, J. D., Catanzarite, D.M., Clair, K.A.S. 1996, "Commercial magneto-rheological fluid devices", International Journal of Modern Physics B, vol. 10, no. 23-24, pp. 2857-2865.

Dogrouz, M. B., Wang, E. L., Gordaninejad, F., Stipanovic, A. J. 2003, "Augmenting heat transfer from fail-safe magneto-rheological fluid dampers using fins", Journal of Intelligent Material Systems and Structures 14 (2), pp. 79-86

Farjoud, A., Vahdati, N., Fah, Y.F., 2008, "MR-fluid yield surface determination in disc-type MR rotary brakes", Smart Materials and Structures, vol. 17, no. 3, art. no. 035021.

Filisko, F.E., Henley, S., 1999, "Flow profiles of electrorheological suspensions: An alternative model for ER activity", Journal of Rheology, Volume 43, Issue 5, pp. 1323-1336.

Foister, R.T., 1997, "Magnetorheological Fluids", US Patent 5,667,715, , General Motors Corporation.

Genc S., Phulé, P.P. 2002, "Rheological properties of magnetorheological fluids", Smart Materials and Structures, vol. 11, no. 1, pp. 140-146.

Genta G., 2002, "Motor Vehicle Dynamics" World Scientific, Singapore,

Gillespie T., 1992, "Fundamentals of Vehicle Dynamics" SAE, Warrendale, PA,.

Gopalswamy, S., 1998, "Magnetorheological Transmission Clutch", US Patent 5,823,309, General Motors Corporation.

Grunwald, A., Olabi, A.G., 2008, "Design of magneto-rheological (MR) valve", Sensors and Actuators A, 148, pp. 211–223.

Jaindl, M., Köstinger, A., Magele, C., Renhart, W. 2007, "Optimal design of a disk type magneto-rheologic fluid clutch", Elektrotechnik und Informationstechnik, vol. 124, no. 7-8, pp. 266-272.

Jolly, M.R., Bender, J.W., Carlson, J.D. 2000, "Properties and applications of commercial magnetorheological fluids", Journal of Intelligent Material Systems and Structures, vol. 10, no. 1, pp. 5-13.

Jolly, M.R., Carlson, J.D., Muñoz, B.C. 1996, "A model of the behaviour of magnetorheological materials", Smart Materials and Structures, vol. 5, no. 5, pp. 607-614.

Karakoc, K., Park, E.J., Suleman, A. 2008, "Design considerations for an automotive magnetorheological brake", Mechatronics, vol. 18, no. 8, pp. 434-447.

Kavlicoglu, B.M., Gordaninejad, F., Evrensel, C.A., Cobanoglu, N., Liu, Y. & Fuchs, A. 2002, "A high-torque magneto-rheological fluid clutch", Proceedings of SPIE - The International Society for Optical Engineering 4697, pp. 393-400.

Klingenberg, D.J. 2001, "Magnetorheology: Applications and challenges", AICHE Journal, vol. 47, no. 2, pp. 246-249.

Li, W.H., Du, H. 2003, "Design and experimental evaluation of a magnetorheological brake", International Journal of Advanced Manufacturing Technology, vol. 21, no. 7, pp. 508-515.

Li, W.H., Du, H., Guo, N.Q. 2003, "Finite element analysis and simulation evaluation of a magnetorheological valve", International Journal of Advanced Manufacturing Technology, vol. 21, no. 6, pp. 438-445.

Liu, B., Li, W.H., Kosasih, P.B., Zhang, X.Z. 2006, "Development of an MR-brake-based haptic device", Smart Materials and Structures, vol. 15, no. 6, pp. 1960-1966.

Ly, H.V., Reitich, F., Jolly, M.R., Banks, H.T., Ito, K., 1999, "Simulations of particle dynamics in Magnetorheological fluids", Journal of Computational Physics 155 (1), pp. 160-177.

Nguyen, Q., Choi, S.. Wereley, N.M., 2008 "Optimal design of magnetorheological valves via a finite element method considering control energy and a time constant", Smart Materials and Structures, vol. 17, no. 2., art. no. 025024

Olabi, A.G., Grunwald, A. 2007, "Design and application of magneto-rheological fluid", Materials and Design, vol. 28, no. 10, pp. 2658-2664.

Rabinow, J., 1951, "Magnetic fluid torque and force transmitting device", US Patent 2,575,360,.

Sukhwani, V.K., Hirani, H. 2008, "Design, development, and performance evaluation of high-speed magnetorheological brakes", Proc. IMechE, Part L: Journal of Materials: Design and Applications, vol. 222, no. 1, pp. 73-82.

Virzì Mariotti G., Lopez F., Triscari F. 2002, "Studio di un ammortizzatore a taratura variabile per una sospensione di autovettura gran turismo" ATA (journal of Associazione Tecnica Automobile), vol 55, n. 5/6, May/June, pp. 188-195, Torino (Italy).

Wiehe, A., Noack, V., Maas, J., 2009, "A Model of Heat Dissipation for MR based Brake", 11th Conference on Electrorheological Fluids and Magnetorheological Suspensions IOP Publishing, Journal of Physics: Conference Series **149** (2009) 012084 doi:10.1088/1742-6596/149/1/012084

Yang, Y., Huang, S.G., Kang, B.S. 2007, "Research on circular plate MR fluids brake", Journal of Central South University of Technology (English Edition), vol. 14, no. 1 SUPPL., pp. 257-259.

Yang, L., Duan, F., Eriksson, A. 2008, "Analysis of the optimal design strategy of a magnetorheological smart structure", Smart Materials and Structures, vol. 17, no. 1.

York, T.M., 1997, "Magnetorheological fluid coupling device and torque load simulator system", US Patent 5,598,908, GSE, Inc.

APPENDIX

1 Determination of performances
Figure 15 shows the simplified draw of the vehicle. F_1 and F_2 represent the braking forces acting respectively on front and rear wheels, P is the vehicle weight applied in the centre of gravity G, while P_1 and P_2 are the contributions of the total weight agents on front and rear carriages respectively. Table 3 shows the main dimensions of the vehicle belonging to the midsize segment.
The contributions of the motion resistances (drag forces and rolling friction of the wheels) and the contribution of the engine braking are neglected in determining the required braking torque. The vehicle is subjected to a constant deceleration (negative) $\dot{u}$, that yields a horizontal inertia force:

$$F = -m \cdot \dot{u} = -fmg \qquad (1A)$$

applied in the centre of gravity, being m the vehicle mass, f the adhesion utilization, g the gravity and neglecting the inertia coefficient. This force causes a weight transfer from rear to the front. Neglecting the effects of suspension of the vehicle (constancy of the position of G in the lack of pitching motions), the dynamic loads P_1 and P_2 are:

$$P_1 = P \cdot \left(\left(\frac{l-x}{l} \right) + \frac{F \cdot h}{P \cdot l} \right) \quad \text{(front)}$$

$$\qquad (2A)$$

$$P_2 = P \cdot \left(\frac{x}{l} - \frac{F \cdot h}{P \cdot l} \right) \qquad \text{(rear)}$$

Usually the manufacturer chooses the braking rate so that the ideal condition:

$$\left(\frac{F}{P}\right)_{max} = f \qquad (3A)$$

f indicates the adhesion utilization of the entire vehicle. Assuming that the values of adhesion utilization are equal for the front and the rear and denoting it by f_0, by (2A) the braking system must be constructed so that:

$$\frac{F_1}{F} = \frac{P_1}{P} = \cos t. = \frac{l-x}{l} + \frac{f_0 \cdot h}{l} \qquad (4A)$$

$$\frac{F_2}{F} = \frac{P_2}{P} = \cos t. = \frac{x}{l} - \frac{f_0 \cdot h}{l} \qquad$$

Being the adhesion utilizations:

$$f_1 = \frac{F_1}{P_1} \qquad f_2 = \frac{F_2}{P_2} \qquad (5A)$$

f_0 is generally assumed equal to 0,6, while R_0 indicates the rolling radius of the tire. By relationships (4A) the braking torque applied to each wheel can be determined:

$$T_1 = \frac{F_1}{2} \cdot R_0 = F \cdot \left(\frac{l-x}{l} + \frac{f_0 h}{l}\right) \cdot \frac{R_0}{2} \quad \text{(front)} \qquad (6A)$$

$$T_2 = \frac{F_2}{2} \cdot R_0 = F \cdot \left(\frac{x}{l} - \frac{f_0 h}{l}\right) \cdot \frac{R_0}{2} \quad \text{(rear)} \qquad (7A)$$

Referring to a situation of braking on dry asphalt with tires in good condition, the adhesion utilization between tire and road is assumed to be equal to $f = 0.8$ into relationship (1A) to exacerbate the solicitation; the wheels do not slide if an anti lock system is mounted on the vehicle. A braking torque on every wheel of the front is obtained equal to 1035,6 Nm, that is taken as reference for the brake design.

2 Preliminary Design

Figure 7 shows a diagram of the configuration adopted, with its geometric parameters. (Sukhwani and Hirani, 2008; Karakoc, Park and Suleman, 2008). In sizing the various components, the first aspect to be considered is the existence of actual limitations of space. In this regard, like the conventional brake, there is the possibility to house the brake inside the rim of the wheel; a limit for the external diameter must be established depending on the diameter of the rim. A minimum value of the difference between outer radius of the cylinder and inner radius of the rim is generally recommended 3 mm, in order to obtain the best utilization of the space. If the rim has diameter of 16", the maximum value of the outer radius of the brake is:

$$R_{max} = [(16 in \times 25.4 mm/in)/2] - 3mm \cong 200mm \qquad (8A)$$

Assuming $\lambda = 0{,}9$ and imposing the required braking torque equal to $T_{nom} = 1036\ Nm$, by relationship (17) one can determine the value of the shear stress that opposes the flowing of MR fluid:

$$\tau(H) = \frac{3T_{nom}}{8 \cdot \pi \cdot (r_e^3 - r_i^3) \cdot \lambda} = 35kPa \qquad (9A)$$

For this value of shear stress, referring to the curves on the MR fluid (Figures 4 and 5), one obtains a value of magnetic induction $H_f=75kA/m$ that determines the maximum magnetic field through the fluid $B_{f,\max} \cong 0,6T$.

Considering the presence of four layers of fluid, having the same gap ξ, by (16) one has:

$$N \cdot I = B_{f,\max} \cdot \frac{4 \cdot \xi}{\mu_f} \qquad (10A)$$

the permeability of MR fluid is considered as constant (linear relationship between B and H) and equal to $\mu_f \cong 5\mu_0$. Considering the maximum current density that a copper wire is capable of carrying, amounting to $J_{\max} = 7A/mm^2$, beyond which excessive heating of the wire is produced, the extent of the cross section of the winding is determined:

$$S_b = \cdot \frac{N \cdot I}{J_{\max} \cdot F_p} = \frac{B_{f,\max} \cdot 4 \cdot \xi}{\mu_f \cdot J_{\max} \cdot F_p} \qquad (11A)$$

Packing factor F_p represents the ratio between the theoretical area occupied by n wires having section S and the effective area S_b ($F_p = (n_0 \cdot S)/S_b$). In the case of wires of circular section is commonly assumed $F_p \cong 0,70$. Choosing an initial value for the thickness of each disc equal to $s_d = 6mm$, i.e., the axial length of the coil is $H_c = 3 \cdot s_d + 4 \cdot \xi = 22mm$.

Table 4 reports all the fixed and calculated quantities in the preliminary sizing. The results are subjected to the approximations introduced with the various simplifying assumptions (linearity and negligible reluctance of the ferromagnetic material).
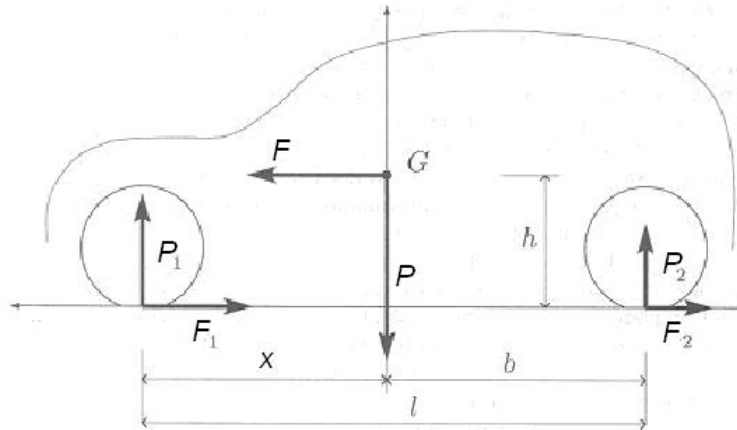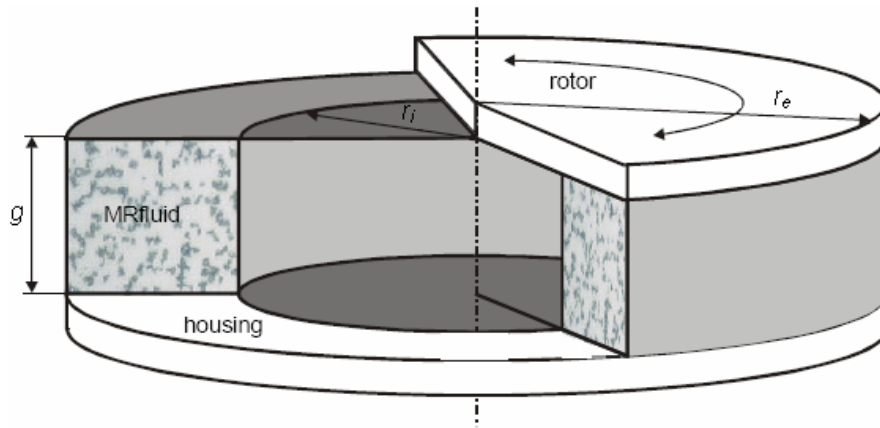

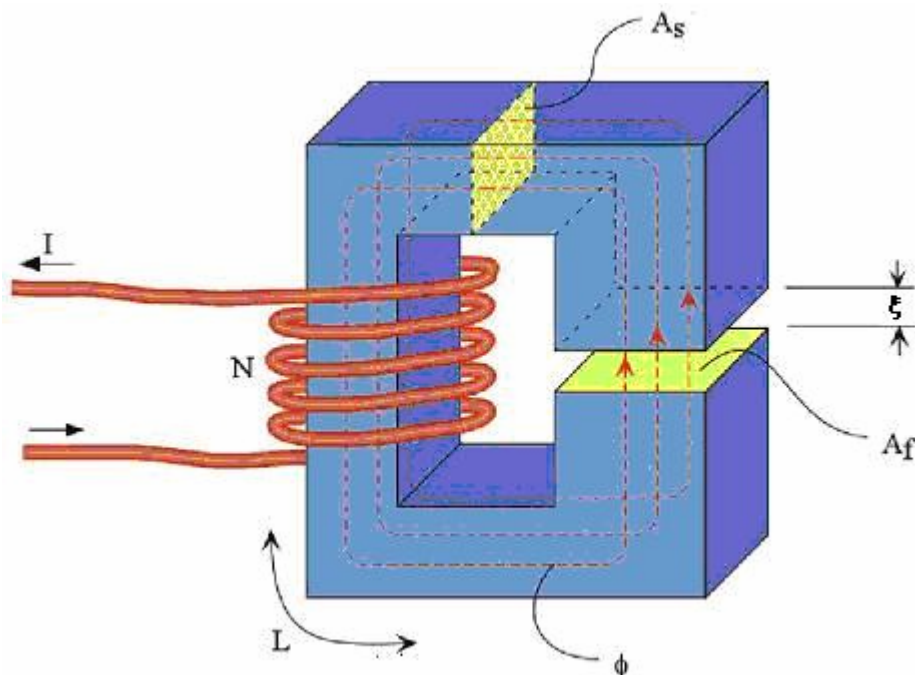**Figure 15** Model of vehicle in braking.

Figure 1 Scheme of a simple MR brake.

Figure 2 - Scheme of magnetic circuit.
N: number of turns; ϕ: magnetic flux; L: length of the iron
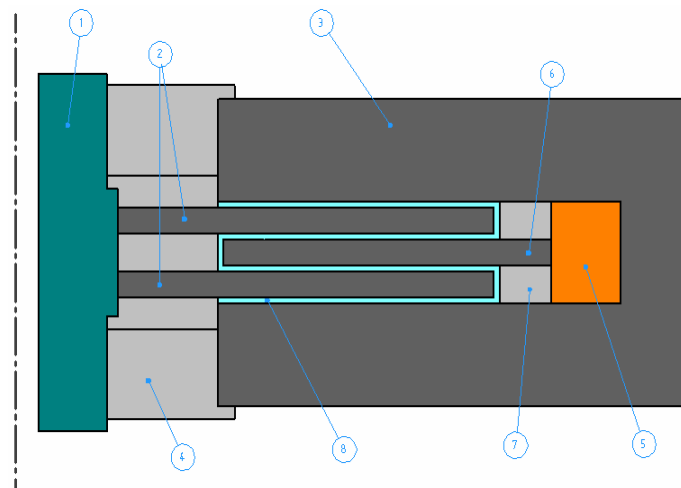
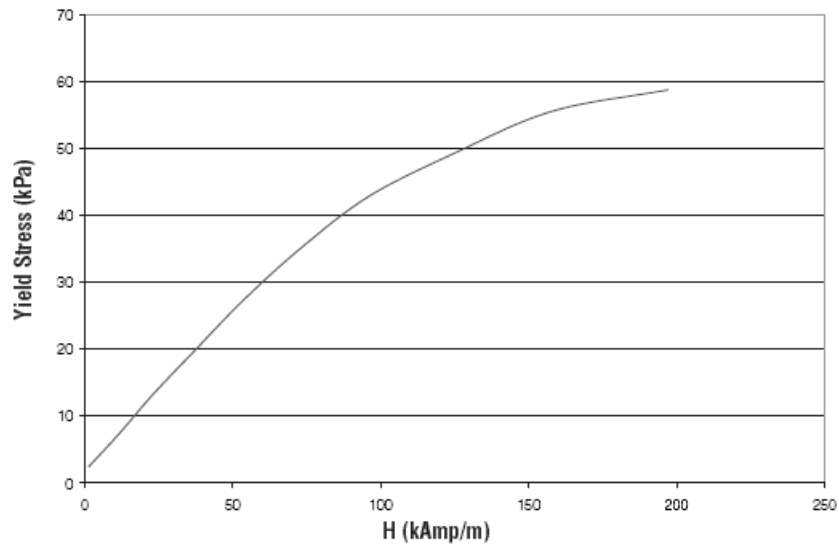

Figure 3 Initial configuration of MR brake.

Figure 4 Shear stress versus magnetic field intensity of the fluid MRF-140CG.
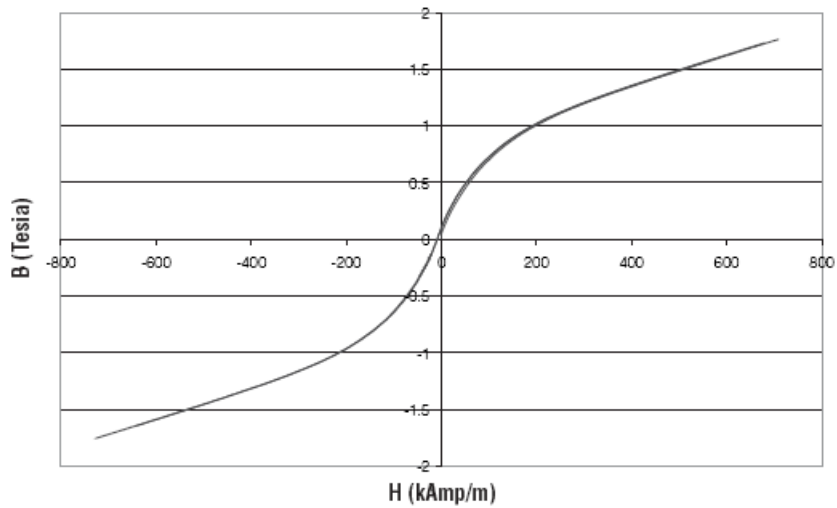

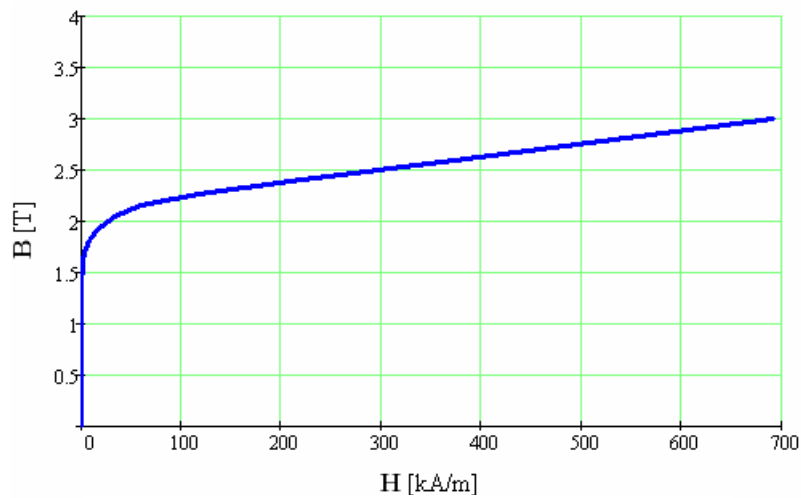**Figure 5** B-H characteristic of the fluid MRF-140CG of LORD Corporation.

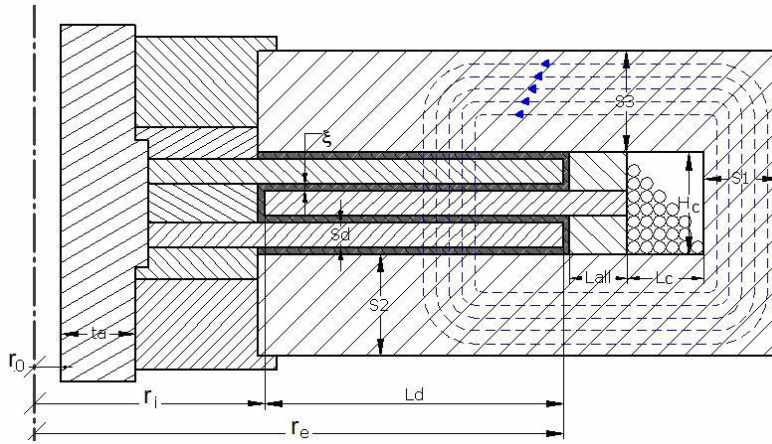**Figure 6** B-H characteristic curve of carbon steel C10.

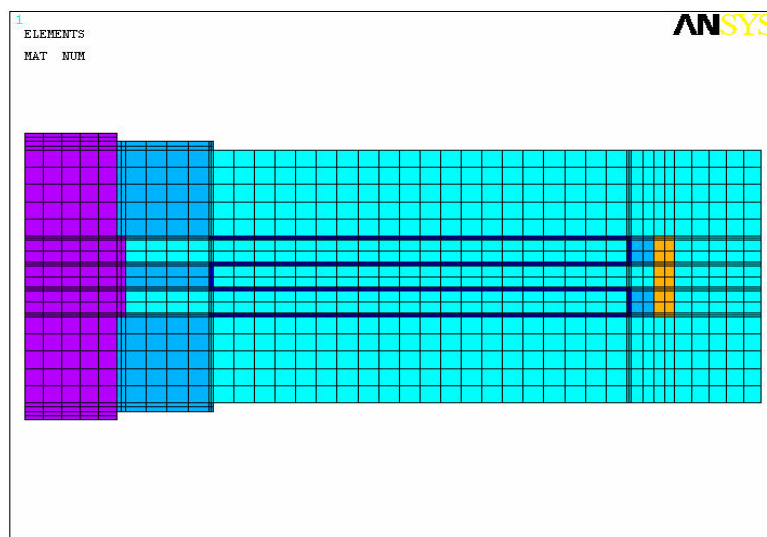**Figure 7** Model of the brake with geometrical parameters.

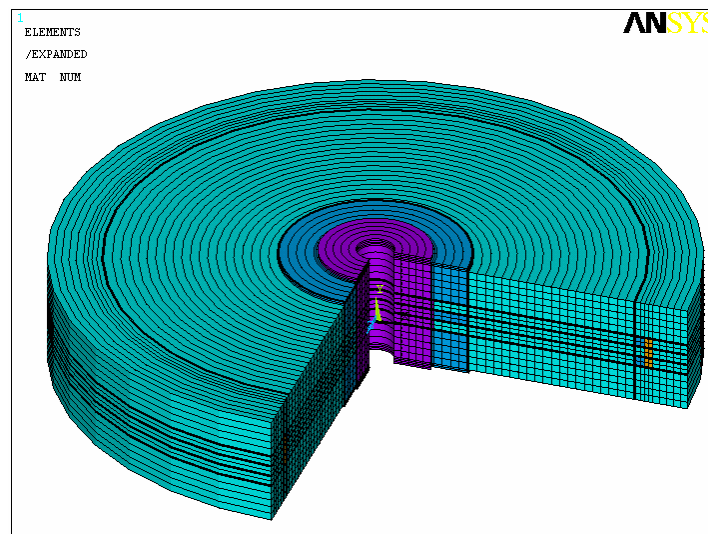**Figure 8** Geometry of MR brake.

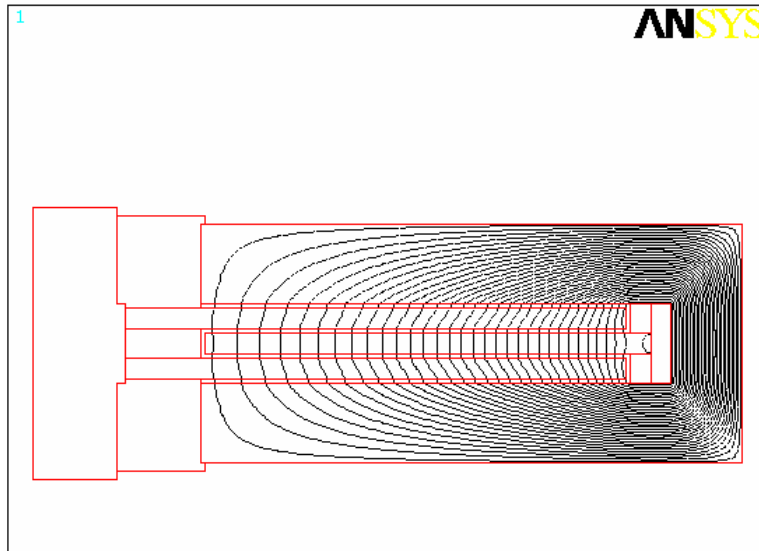**Figure 9** Three-dimensional FEM model.

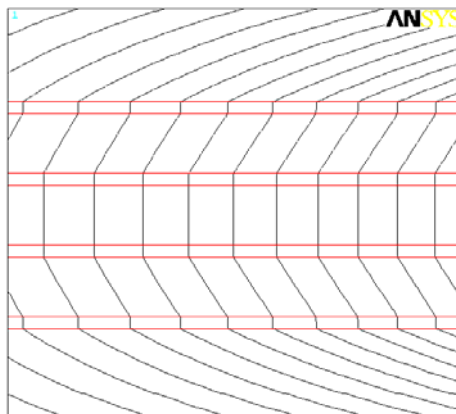**Figure 10** Flow lines in the MR brake.

Figure 11 Magnification in correspondence of the fluid gap.
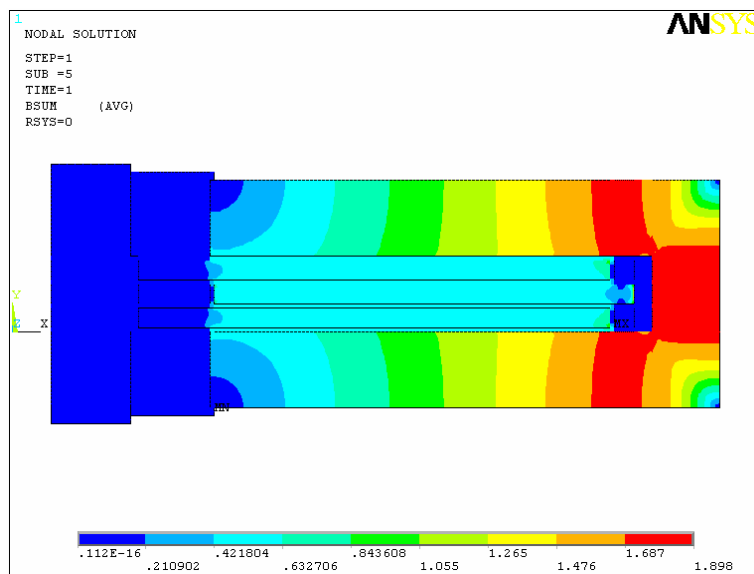
Figure 12 Distribution of the magnetic field in MR brake.
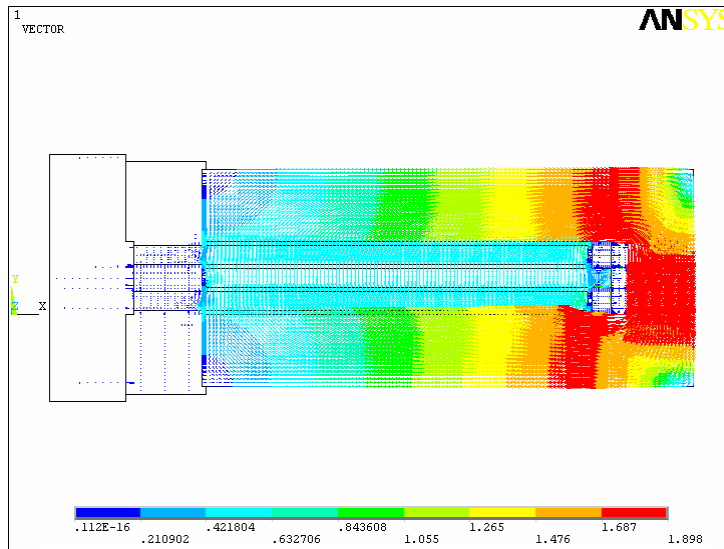
Figure 13 Vector representation of the magnetic field B.

Figure 14 Magnetic field intensity H in the MR brake.

Table 1 Physical properties of fluid MR140CG LORD Corporation.

Properties MR-140CG	
Base Fluid	Oil hydrocarbon
Color	Dark gray
Working temperature (°C)	-40 - 130
Viscosity (Pa·s)	0,280
Density (kg/m^3)	3540
Weight percentage of particles	85,44%

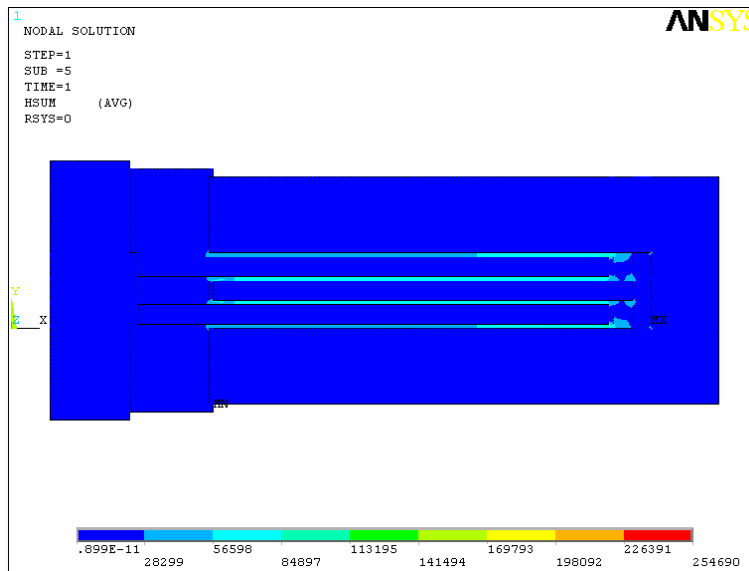Table 2 Main properties of the brake materials.

Properties	C10	AISI 304	Al T6061-T6	Copper (of the coil)
Composition	C 0,08-0,13% Fe 99,1-99,6% Mn 0,3-0,6%	C 0,08% Cr 18-20% Fe 66-74% Mn 2% Ni 8-10,5%	Al 95,8-98,6% Cr 0,04-0,35% Cu 0,15-0,4% Fe 0,7% Mg 0,8-0,2%	
Density (kg/m^3)	7860	8000	2700	
Yield strength (MPa)	305	215	276	
Ultimate strenght (MPa)	365	505	310	
Elastic modulus (GPa)	205	193	68,9	
Poisson ratio	0.29	0.29	0,33	
Thermal Conductivity ($W/m \cdot K$)	49,8	16,2	167	140
Specific heat ($J/Kg \cdot °C$)	448	500	896	385

Table 4. Preliminary Design

Item (fig, 9)	symbol	quantity	reference
Maximum radius of the brake	R_{max}	200 mm	
Coefficient of correction	λ	0,9	
Number of active surfaces	n	4	
Ring thickness	L_{all}	5 mm	
Disk external radius	r_e	160 mm	
Disk internal radius	r_i	55 mm	
Inner radius of the shaft	r_0	10 mm	
Shaft thickness	t_a	20 mm	
Radial extension of the active surface	L_d	100 mm	
Thickness of MR fluid	ξ	1 mm	0,25 – 2 mm
Packing factor	F_p	0,7	
Effective area of N wires	S_b	78 mm^2	by (25)
Thickness of every disc	s_d	6 mm	
Axial length of the coil	H_c	22 mm	
Coil extension in radial direction	L_c	3,5 mm	
Magnetomotive force	N I	382 Amp-turns	by (24)
Number of turns	N	254	
Thickness of outer casing	S_1	19 mm	
"	S_2	22 mm	
"	S_3	22 mm	
Shear stress	$\tau(H)$	36 kPa	by (23)
Magnetic induction	H_f	95 kA/m	Fig. 6
Magnetic field	$B_{f.max}$	0,6 T	Fig. 7
Maximum current density in a copper wire	J_{max}	7 A/mm^2	
Magnetic permeability of the vacuum	μ_0	$4\pi\ 10^{-7}$ N/A^2	
Magnetic permeability of MR fluid (first approximation)	$5\ \mu_0$	$20\pi\ 10^{-7}$ N/A^2	

Table 3 Details of the vehicle model.

Vehicle Features	
Type of drive	front wheel
Tires	195/45 R16
Mass (Kg)	m=1300 Kg
Wheel base	l=2,5 m
CG height	h=0,5 m
Diameter of the wheel rim	16" (0.4064 m)
Tire rolling radius	R_0=0,282 m
% static load distribution rear	x/l=40%
% static load distribution front	(l-x)/l=60%

NOMENCLATURE

A	generic area
A_f	active surface
A_s	section of the branch s of the circuit
A_z	magnetic potential vector
B	magnetic field
B_f	working point of magnetic field
B_{fmax}	maximum value of the magnetic field
B_s	magnetic field in the branch s of the circuit
f	adhesion utilization
f_0	design value of adhesion utilization
f_1	adhesion utilization on the front
f_2	adhesion utilization on the rear
F	braking force
F_1	braking force on the front
F_2	braking force on the rear
F_p	packing factor
g	gravity acceleration
h	height of the gravity center
H	magnetic field intensity
H_c	axial lenght of the coil
H_f	working value of magnetic field intensity
H_s	magnetic field intensity in the branch s of the circuit
I	current
j	index of the generic node
J	current density
J_{max}	maximum value of the current density in a wire
l	wheelbase of the vehicle
L	generic lenght
L_{all}	Ring thickness
L_c	coil extension in radial direction
L_d	radial extension of the active surface
L_s	lenght of the generic branch s of the circuit
m	mass of the vehicle
m_b	mass of the brake
n	number of active surfaces
n_0	number of wires
n_1	number of nodes on every active surface
N	number of turns of the coil

N I	magnetomotive force
P	weight of the vehicle
P_1	weight of the vehicle on the front
P_2	weight of the vehicle on the rear
r	generic radius of the disk
r_e	esternal radius of the disk
r_i	internal radius of the disk
r_j	radius of the generic node j
r_0	inner radius of the shaft
R_{max}	maximum radius of the brake
R_0	rolling radius of the wheels
s	index of the branch of the magnetici circuit
S	area occupied by n wires
S_b	cross section of the winding
s_d	thickness of one disk
S_1, S_2, S_3	thicknesses of outer casing
t_a	shaft thickness
T	torque moment
T_H	torque moment due to magnetic field
T_{nom}	torque moment of calculation
T_η	torque moment due to viscosity variation
T_1	torque moment on every wheel of the front
T_2	torque moment on every wheel of the rear
$\dot{u}$	vehicle deceleration
W	surface contained by close curve Z
x	distance of the gravity center by the front
Z	generic closed curve
$\dot{\gamma}$	tangential velocity gradient
η	viscosity
θ	angular coordinate
λ	correction coefficient
μ	permeability
μ_0	permeability of the vacuum
μ_f	permeability of the fluid
μ_r	relative permeability
τ	tangential stress
τ_H	tangential stress due to magnetization of the fluid
τ_j	tangential stress at the generic node j
τ_y	yield stress
ω	angular velocity
ϕ	magnetic flux
ξ	gap of fluid
$\Re$	magnetic reluctance
$\Re_f$	reluctance of gap fluid
$\Re_s$	reluctance of the ferromagnetic material